Small-angle attraction in the tilt illusion

Ayşe Akgöz

Integrated Program in Neuroscience

McGill Vision Research, Department of Ophthalmology and Visual Sciences

McGill University, Montreal

December 2021

A thesis submitted to McGill University in partial fulfillment of the requirements of the degree of Master of Science

Contents

Abstract

The tilt illusion defines the phenomenon in which a surround or inducer grating of a particular orientation impacts the perceived orientation of a central test grating. Typically, inducer-test orientation differences of 5-40 deg drive the test grating orientation to appear shifted in a direction away from that of the inducer orientation, i.e., show repulsion. The inducer typically causes the test grating orientation to appear shifted towards that of the inducer orientation in the region 60-90 deg, i.e. shows attraction. Both repulsion and attraction effects have been observed in contrast-modulated and luminance-modulated grating patterns. In this thesis, I demonstrate that a secondary, small-angle (0-10 deg) attraction effect is observed in contrast-modulated and orientation-modulated gratings, as well as with luminance-modulated gratings that are relatively low in spatial frequency low in contrast or contain added micropattern texture. The observed small-angle attraction, which in some instances exceeds in magnitude the repulsion and the aforementioned large-angle attraction effects, is dependent on the spatial phase relationship between the inducer and test, being maximal when the center and surround are in in-phase condition. Both small-angle attraction and repulsion effects are reduced when a gap is introduced between test and inducer. My findings suggest that small-angle attraction in the Tilt Illusion is likely a result of the blending or assimilation of the receptive fields of the neurons sensitive to the inducers and tests when those are similar in orientation.

Résumé

L'illusion d'inclinaison définit le phénomène par lequel un réseau périphérique ou incitateur affecte l'orientation perçue d'un réseau test central. Typiquement, une différence d'orientation incitateur-test de 5-40 deg entraîne l'orientation du réseau test à apparaître éloignée de celle de l'incitateur, c'est-à-dire une répulsion. L'incitateur cause typiquement l'orientation du réseau test à apparaître décalée vers celle de l'incitateur dans la région 60-90 deg, c'est-à-dire une attraction. Des effets de répulsion et d'attraction ont tous deux étés observés avec des réseaux de modulation de contraste et de modulation de luminance. Dans cette thèse, nous démontrons qu'un effet d'attraction secondaire, avec un petit-angle (0-10 deg) est observé avec des réseaux de modulation de contraste, de modulation d'orientation ainsi que de modulation de luminance qui sont présentés à de relativement basses fréquences spatiales, bas contraste ou contiennent des textures de micropatterns additives. L'attraction de petit-angle observée, qui dans certains cas excède la magnitude des effets de répulsion et d'attraction à grand-angle susmentionnés, est dépendante de la relation spatiale de phase entre l'incitateur et le test, étant maximale lorsque le centre et la périphérie sont en phase. Les effets d'attraction à petit-angle et de répulsion sont tous deux réduits lorsqu'un intervalle est introduit entre le test et l'incitateur. Nos résultats suggèrent qu'une attraction à petit-angle dans le TI est probablement le résultat d'un assemblage ou d'une assimilation des champs récepteurs des neurones sensibles aux incitateurs et tests lorsque ceux-ci sont d'orientation similaire.

Acknowledgements

I am grateful to my supervisor, Dr. Frederick Kingdom for his support, training, and for sharing his expertise throughout my candidature. I would like to thank Dr. Elena Gheorghiu at Stirling University for her contribution to the research, both as an academic collaborator and test observer. Special thanks to Drs. Alex Baldwin and Curtis Baker for their mentorship and insights as members of my advisory committee. Thanks also to Dr. Alexandre Reynauld for translating the thesis abstract into French. Finally, I would like to thank my family for their endless support, as well as my two best-friend psychologists Havagül Akçe and Munir Bauer for helpful discussions and friendship throughout my time at McGill.

Over the course of my degree, my stipend has been supported by funding from the Natural Sciences and Engineering Research Council (NSERC) grants to Dr. Frederick Kingdom.

Contribution of Authors

The main experimental chapter of this thesis (Chapter 2) contains a manuscript which is intended to be submitted to the Journal of Vision by Ayşe Akgöz, Frederick Kingdom, and Elena Gheorgiou. AA designed the experiments in collaboration with EG and FK, and AA collected and analyzed the data. AA wrote the first draft of the thesis, which was then edited and refined by FK.

Chapter 1: Introduction and Literature Review

Background

Visual perception is the sensory ability that utilizes the light in the visible spectrum reflected from objects to our eyes. However, what we see is not an exact copy of the retinal stimulus. Researchers interested in perception have therefore attempted to explain how the visual input translates to our internal sensory experience. The differences between perception and reality are most pronounced in the class of phenomena termed visual illusions, of which the tilt illusion (TI) explored in this thesis and shown in Figure 1.1 is an exemplar. Visual illusions such as the TI are typically defined as a "discrepancy between perception and reality" (Gillam, 1998; Gregory, 2004; Wade, 2005), although precise views on what constitutes a visual illusion differ (Gillam 1998; Gregory 2004; Wade 2005). Here we use the definition that an illusion is a "divergence between perception and reality that stands out as an anomaly" the definition that Kingdom (2015) attributes to the vision scientist Dejan Todorovic.

Richard Gregory classified visual illusions into three main classes: physiological, physical, and cognitive illusions, each containing four illusion types: ambiguities, distortions, paradoxes, and fiction (Gregory, 1997). In Gregory's scheme, physical illusions are caused by the physical environment, for example, by the optical features of light reflection on water, such as with mirages. Physiological illusions occur in the eye and/or the visual pathway, e.g., from the effects of stimulation of retinal neurons, for example the negative afterimages caused by exposure to colored lights. Cognitive visual illusions are caused by unconscious inferences, which, according to Gregory, explain many geometric distortions such as the well-known Müller -Lyre illusion (Müller-Lyre, 1889).

Context and the tilt illusion

Context influences many aspects of visual perception. For example, a grey patch appears darker when surrounded by a brighter compared to a darker stimulus, the phenomenon known as simultaneous brightness contrast (Hering, 1874/1964). The related phenomenon of simultaneous contrast-contrast is said to occur when the perceived contrast of a texture or grating is lowered when surrounded by a higher-contrast version of the same type of texture or grating (Chubb et al., 1989; Cannon and Fullenkamp, 1991; Snowden and Hammett, 1998; Xing and Heeger, 2000). Context can be temporal as well as spatial: prolonged inspection of a moving object results in a subsequently presented static object appearing to move in the opposite direction – the well-known motion aftereffect. The TI studied here, like the simultaneous effects described above, is a well-studied example of the effect of a surround on the perceived properties of a central test stimulus. Contextual effects in general provide important clues as to the underlying mechanisms of visual perception, as we shall now see in relation to the TI.

Mechanisms of the tilt illusion

In the classical TI, two examples of which are shown in Figure 1.1., an obliquely tilted inducing grating induces the perceived orientation of a vertical test grating to be slightly tilted in the opposite direction, an example of a “repulsive” interaction, and this effect maximally occurs for inducer-test orientation differences of around 15-20 deg. The classical explanation of this repulsive effect in the TI is lateral inhibition between orientation-selective neurons (Wallace, 1969; Blakemore, Carpenter & Georgeson, 1970; Tolhurst and Thompson, 1975; Ringach, 1997). For any given stimulus orientation, the distribution of responses from orientation-tuned neurons is typically a normal distribution whose peak response is given by the neuron whose preferred orientation is the same as that of the stimulus orientation. Perceived stimulus orientation is believed to be encoded by some measure of the distribution's central tendency, such as the mean or mode. In the TI stimulus, the orientations of the inducer and test are different. Therefore, their neural response distributions will have different peaks but overlap. Suppose the inducer-responsive neurons inhibit the test-responsive neurons. In that case, the resulting distribution of neural responses to the test grating will become skewed away from the responses to the inducer grating. The result is that the perceived orientation of the test is shifted away from its standard value obtained with no surround.

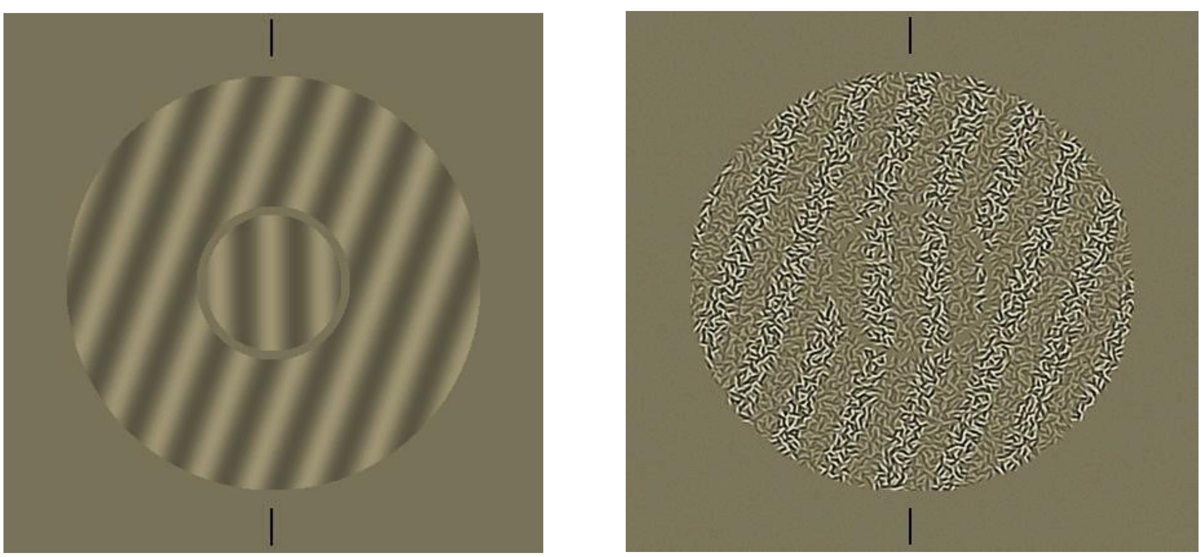

Figure 1.1. Tilt illusion with 1st-order LM (luminance modulated) and 2nd-order CM (contrast modulated) stimuli. The bars in the central test area are physically vertical, but for most observers appear slightly tilted counterclockwise.

A number of studies have also found that around an angular difference of 70 deg the orientation of the test is shifted towards rather than away from the inducer (e.g., Over, Broerse, & Crassini, 1972; Wenderoth & Johnstone, 1987; reviewed by Clifford, 2014). This "large-angle attraction" in the TI has been attributed to disinhibition (Clifford, 2014) but there are other accounts. Based on the finding that large-angle attraction effects are subject to different spatio-temporal dependencies compared to the repulsion effect, some authors have suggested that large-angle attraction is mediated by higher striate areas where orientation constancy mechanisms are involved (Wenderoth and Johnstone, 1987, 1988; Zwan and Wenderoth, 1994, 1995; Smith and Wenderoth 1999). Consistent also with this account is the evidence from Tomassini & Solomon (2014) that large-angle attraction requires conscious awareness, though an earlier report by Mareschal & Clifford (2012) suggests otherwise.

First- and second-order stimuli

This thesis measures the TI with both 1st-order as well as 2nd-order stimuli, so it is worth examining the differences between the two stimulus dimensions. With 1st-order stimuli, such as modulations in luminance or color, there is a peak in the Fourier amplitude spectrum at the modulation frequency, whether measured over space or time. Moreover, it is believed that such stimuli are detected in the cortex by linear or quasi-linear neurons whose receptive-field sub-regions are responsive to changes in luminance or color, such that the neuron as a whole is sensitive to luminance or color contrasts at its preferred modulation frequency. 2nd-order stimuli on the other hand are stimuli whose signature modulations, while distinguishable by human observers, produce no peaks in Fourier energy at the scale of the modulation. The modulations in these stimuli are therefore undetectable by linear neurons tuned to the modulation frequency.

This is because the local undulations in luminance that define the carrier of the stimulus would cancel within the 2^{nd}-order-sensitive neurons receptive-field sub-regions.

Bergen and Adelson (1988) were the first to suggest a general-purpose computational model for detecting 2^{nd}-order stimuli, or specifically the sharp texture boundaries that have been identified with the effortless segregation of textures. Generically termed "the back-pocket model" of texture segregation (Chubb & Landy, 1991), the model consists of three stages: filter, rectify, filter (FRF; also known as LNL for linear, nonlinear, linear). The first linear spatial filter is tuned for orientation and spatial frequency; it is responsive preferentially to one of the two texture regions either side of the texture edge. A spatial average of these linear filter responses will be the same on each side of the texture edge. After this step, a "second-order" linear filter responds strongly to the texture-defined edge. The kinds of image structure described by FRF models are pretty common in natural images and is not correlated with first-order structure (Schofield, 2000).

2^{nd}-order stimuli come in many varieties: they can be made from alternating modulations of features such as local contrast, orientation, density, binocular disparity and motion (Baker 1999; Langley et al. 1996; Lin and Wilson 1996; Wilson et al. 1992). The most commonly used second-order visual stimulus is the one characterized by modulations of local contrast, termed contrast-modulated or CM. The example CM stimulus in Figure 1.1 consists of a relatively low modulation spatial frequency, termed the envelope, of relatively higher spatial frequency luminance-defined Gabor micropatterns, termed the carrier. In this thesis, besides making measurements of the TI in CM gratings I also measure the TI for orientation-modulated, or OM gratings (Kingdom, Keeble & Moulden, 1995) in order to test the generality of our results. An example OM grating is shown in the following chapter.

It is broadly accepted that 2nd-order stimuli at modulation detection threshold are detected by separate visual mechanism from their 1st-order luminance modulated (LM) counterparts (Schofield & Georgeson, 1999; Cruickshank and Schofield, 2005. The psychophysical evidence for separate mechanisms for 1st- and 2nd-order stimuli is complemented by neurophysiological findings (Baker 1999; Mareschal and Baker 1998a; Mareschal and Baker 1998b). However, one study have discovered a degree of cross-adaptation between first-order LM and second-order CM and OM stimuli, suggesting a common underlying mechanism (Filangieri & Li, 2009).

Brain imaging studies of 1st and 2nd-order stimuli

Brain imaging studies have been used to elucidate the extent to which 1st- and 2nd-order stimuli are processed separately. Many fMRI (functional magnetic resonance imaging) studies have attempted to find significant associations of particular brain areas for texture, i.e. 2nd-order processing tasks. For example, investigators have found brain areas strongly responsive to the texture of an object or adaptative for a newly seen texture (Cant, Arnott, & Goodale, 2009; Cavina-Pratesi, Kentridge, Heywood, & Milner, 2010a; 2010b; Stylianou-Korsnes, Reiner, Magnussen, & Feldman, 2010). Consistent with neurophysiological findings, these studies are indicative of the involvement of various brain areas in texture processing, including the posterior collateral sulcus and the right inferior parietal lobe.

In one of many types of fMRI methods an “adaptation index” is used to measure the decline in response to same frequency or orientation of modulation in comparison to adaptation to a different type of modulation. If the response decline is greater for same compared to different modulation types this is taken as evidence for separate mechanisms. The method has demonstrated that second-order orientation and spatial frequency tuning occurs in several visual cortical areas (Hallum, Landy, & Heeger, 2011; Larsson et al., 2006; Montaser- Kouhsari, Landy, Heeger, & Larsson, 2007). According to these studies, the "adaptation index" increases from V1 through downstream visual areas, with consistent orientation-selective adaptation to CM, OM, and LM patterns observed in V1, V2, V3, V3A/B, LO1, hV4, and VO1 (Larsson et al., 2006). For first-order (LM) patterns on the other hand, adaptation was no stronger in downstream areas than in V1. These findings are consistent with the "gradualist encoding" approach of El-Shamayleh and Movshon (2011) who suggested that tuning for 2nd-order patterns might "gradually" arise across different cortical regions instead of all at once in area V2.

Taken together these brain imaging studies add further support to the idea that 1st- and 2nd-order patterns are, at least partially processed by separate mechanisms. What then of the evidence for 2nd-order tilt illusions and whether or not they are processed separately from 1st order tilt illusions?

2nd-order tilt illusion

Although traditionally the TI has been demonstrated using luminance-modulated, or LM gratings, Smith et al. (2001) demonstrated the TI in a contrast-modulated, or CM stimulus, an example of which is shown alongside its LM counterpart in Figure 1. They also measured the interaction between LM and CM stimuli in the TI, in other words what happens when one type of modulation defines the inducer and the other the test. In so doing they considered to what extent the TI is underpinned by a generic mechanism that enjoys common support from both "1st-order" LM and "2nd-order" CM stimuli (see below). They demonstrated repulsion and large-angle attraction effects with the CM gratings only slightly less than those obtained with LM gratings, with the maximum repulsion at 15 degrees, and the maximum large-angle attraction effect at 75 degrees. Importantly they then found that the magnitude of the TI was similar for all combinations of inducer and test, i.e., for LM-LM, CM-CM, CM-LM, LM-CM, in keeping with a common TI mechanism for both 1st- and 2nd-order stimuli. This evidence for a common mechanism underpinning both 1st- and 2nd-order TIs would seem at odds with some, but by no means all of the aforementioned evidence for the separability of the processing of the two stimulus dimensions.

Why a new study of the tilt illusion?

The repulsion and large-angle attraction effects in the TI reported in almost all studies have been based on measurements of inducer-test angles typically in the range 5-90 deg, with repulsion observed for angles <50 deg and attraction for angle >50 deg. What happens however when the inducer and test patterns have very similar orientations, e.g., <10 deg apart? Takeo, Watanabe & Clifford (2020) found evidence for attraction in LM gratings with 10 deg inducers, but only at very short stimulus durations, specifically 20ms or less. Mareschal, Morgan & Solomon (2010), using stimuli comprised of a central Gabor test surrounded by four Gabor flankers found attraction for 5-10 deg flanker-test differences, but only at an eccentricity of 10 deg. These two studies hint at the possibility of small-angle attraction in the TI, but they are reinforced by studies that while not directly measuring the TI are close relatives. Using orientationally-narrowband noise patterns Blake, Holopigian, and Jauch (1985) measured a test noise pattern's perceived orientation in the context of a superimposed mask noise pattern. They found that at large angular orientation differences (>10 deg), the test orientation appeared rotated away from the mask orientation, the overlay masking equivalent of the repulsive effect in the TI. However, observers in the study had difficulty distinguishing between test and noise orientations when the two patches were within 5 degrees of one another. If the test and mask orientations were < 10 deg, the test orientation appeared rotated towards the mask orientation. It is not clear how the inhibitory interactions between channels with very different orientation that accounts for repulsion affects in such things as overlay masking and the TI would account for this “reverse illusion”. Presumably instead the form of neural activity produced by a pair of different orientations differing by just a few degrees resembles the pattern of activity produced by a single orientation situated somewhere between the pair. Thus in Blake et al.s study, when the test and noise patch orientations were within 5-10 degrees of one another, the test grating appeared pulled slightly towards the orientation of the noise, an example of what we term here a “small-angle” attraction effect. The overlay masking in Blake et al.s study is presumably underpinned by mask and test mechanisms with similar receptive field characteristics to the inducer and test receptive fields involved in the TI suggesting that a similar attraction effect for minor inducer-test orientation differences might also be expected in the TI.

Further support for the possibility of small-angle attraction in the TI comes from a study by Motoyoshi and Kingdom (2003). They required test subjects to discriminate noise patterns consisting of an even distribution of orientation energy from patterns with orientation energy sinusoidally modulated across orientation (i.e. not across space or time). They found that sensitivity was bandpass with respect to orientation frequency and modelled their results with an orientation-based filter that involved facilitatory, i.e. attractive interactions between similar orientations, and inhibitory, i.e. repulsive interactions between dissimilar orientations.

Any such small-angle attraction effect might intuitively be expected to be dependent on the spatial phase relationship between inducer and test modulations. At slight orientation differences, the modulation bars of the inducer and test are close to colinear. If the receptive fields of the inducer- and test-sensitive neurons overlap, we might expect summation when they are in-phase and cancellation when out-of-phase. The spatial-phase relationships between inducers and tests have not to our knowledge ever been manipulated in TI studies, so the experiments described in this thesis will consider spatial phase as an independent variable.

Lastly, we might expect small-angle attraction to be dependent on the spatial-frequencies of the inducers and tests, since for a given test area the receptive field sizes of the neurons sensitive to the inducers/tests will increase, and hence the amount of their overlap with increase, as spatial-frequency decreases. Therefore we have also considered the effects of spatial frequency on the TI, for both small and large angles.

Rationale of thesis

This thesis aims to explore contextual influences in texture perception using the well-known tilt illusion, or TI. The rationale for the experiments in this thesis is that there are *a priori* grounds for supposing that there might be a general attraction effect in the TI for small inducer-test angles. While there are hints in the previous literature as to the existence of small-angle attraction in the TI, the TI has not been measured in any systematic detail in the region <10 deg. In summary, the aims are to measure the TI across the full range of inducer-test angles, in detail in the range <10deg, for both 1st-order and 2nd-order grating stimuli, and for a range of parameters such as modulation spatial-frequency, modulation waveform-type and gap size.

Chapter 2

Manuscript to be submitted to *Journal of Vision*

Small-angle attraction in the tilt illusion

Ayşe Akgöz, Elena Gheorghiu* and Frederick A. A. Kingdom

McGill Vision Research, Department of Ophthalmology, Montréal General Hospital

1650 Cedar Ave. Rm. L11.512, Montréal, Québec, H3G 1A4

*Department of Psychology, University of Stirling, Stirling, Scotland, United Kingdom

Abstract (as in the thesis abstract)

The tilt illusion describes the phenomenon in which a surround, or inducer grating of a particular orientation influences the perceived orientation of a central, test grating. Typically, inducer-test orientation differences of 5-40 deg cause the test grating orientation to appear shifted in a direction away that of the inducer orientation, i.e. shows repulsion. In the region 60-90 deg, the inducer typically causes the test grating orientation to appear shifted towards that of the inducer orientation, i.e. shows attraction. Both repulsion attraction effects have been observed in contrast-modulated as well as luminance-modulated grating patterns. Here we show that a secondary, small-angle (0-10 deg) attraction effect is observed in contrast-modulated and orientation-modulated gratings, as well as with luminance-modulated gratings that are relatively low in spatial frequency, low in contrast or contain added micropattern texture. The observed small-angle attraction, which in some instances exceeds in magnitude the repulsion and the aforementioned large-angle attraction effects, is dependent on the spatial phase relationship between the inducer and test, being maximal when in-phase. Both small-angle attraction and repulsion effects are reduced when a gap is introduced between test and inducer. Our findings suggest that small-angle attraction in the TI is likely a result of the blending, or assimilation of the receptive fields of the neurons sensitive to the inducers and tests when similar in orientation.

Keywords: tilt illusion, tilt induction, 2nd-order, texture, surround inhibition, assimilation, attraction

Introduction

The tilt illusion, or TI, first reported by Gibson (1937), is the phenomenon in which the perceived orientation of a central test line or grating is altered by the presence of a surround or inducing line/grating of a different orientation (see review by Clifford, 2014). Examples of the TI are shown in Fig. 1. The figure includes not only luminance-defined (LM) or "1st-order" gratings but two types of texture-defined, or "2nd-order" gratings: contrast-modulated (CM), for which the TI has also been demonstrated (Badcock & Hutchison, 1998; Smith, Clifford & Wenderoth, 2001), and orientation-modulated (OM) which to our knowledge has not. In the classical version of the TI with LM stimuli, an obliquely tilted inducing grating or line causes the perceived orientation of a vertical test grating or line to be slightly tilted in the opposite direction. This "repulsive" interaction occurs maximally for inducer-test orientation differences of around 15-20 deg. Inducer gratings 70 deg or more away from the test grating typically cause the test grating to appear tilted *towards* the inducer orientation, with the maximum effect observed between 75 and 80 deg and termed the "indirect" effect (Over, Broerse, & Crassini, 1972; Wenderoth & Johnstone, 1987; Clifford, 2014). Here we use the term large-angle attraction for this effect to distinguish it from the potential small-angle attraction effect that the present study aims to investigate.

The classical explanation of the repulsive effect in the TI is lateral inhibition between orientation selective neurons (Wallace, 1969; Blakemore, Carpenter & Georgeson, 1970; Georgeson, 1973; Tolhurst and Thompson, 1975; Ringach, 1997; Clifford, 2014). For the large-angle attractive effect, disinhibition, i.e. "inhibition of the inhibition" (Clifford, 2014) and orientation constancy (Wenderoth & Johnstone, 1987, 1988) have been suggested as possible explanations, explanations to which we shall later return.

In this communication we explore the TI in some detail at small angles, specifically in the region 0-10 deg, to determine whether or not there is a secondary, small-angle attraction effect distinct from the large-angle attraction effect discussed above. Why study the TI at small angles? First, few studies have delved into 0-10 deg TI territory. Second, of the papers that have, only two to my knowledge have found evidence for small-angle attraction and then only in very limited circumstances. Takeo, Watanabe & Clifford (2020) found small-angle TI attraction in LM gratings with 10 deg inducers, but only at very short stimulus durations, specifically 20ms or less. Mareschal, Morgan & Solomon (2010), using stimuli comprised of a central Gabor test surrounded by four Gabor flankers found small-angle attraction for 5-10 deg flanker-test differences, but only at an eccentricity of 10 deg. Other non-TI studies are supportive of the possibility of small-angle attraction in the TI. Using orientationally-narrowband noise patterns, Blake, Holopigian and Jauch (1985) measured the perceived orientation of a test noise pattern in the context of a superimposed mask noise pattern. They found that at large mask-test angles (>10 deg) the test orientation appeared rotated away from the mask orientation, in keeping with repulsion effect in the TI. However, when mask-test angles were < 10 deg the test orientation appeared rotated towards the mask orientation, showing attraction. Given that overlay masking is likely underpinned by similar mechanisms as do mediate the TI, we might expect a similar attraction effect in the TI. Further support for the possibility of small-angle attraction in the TI comes from a study by Motoyoshi and Kingdom (2003). They required test subjects to discriminate noise patterns with an even distribution of orientation energy from ones with orientation energy that was sinusoidally modulated across orientation, rather than across space or time. They found that sensitivity was bandpass with respect to orientation frequency and modelled their results with an orientation-based filter that involved facilitatory, i.e. attractive interactions between similar orientations, and inhibitory, i.e. repulsive interactions between dissimilar orientations.

One reason why small-angle attraction may have proved elusive in standard TI protocols is that the spatial-phase relationship between inducer and test has not been an independent variable. If small angle attraction were to be dependent on colinear interactions between inducer and test we might expect it to be dependent on their spatial-phase relationship. To this end I have measured the TI at small angles using modulations in which the spatial phases of inducer and test have been either in-phase or anti-phase.

Methods

Participants

The three authors acted as observers. An undergraduate volunteer was also used for one of the experiments as fourth participant (Experiment 4). All subjects were emmetropic or wore corrective lenses. All experiments were conducted in accordance with the Declaration of Helsinki and the Research Institute of theMcGill University Health Centre (RI-MUHC) Ethics Board. Observer initials on graphs have been anonymized in accordance with requirements of the (RI-MUHC) Ethics Board.

Apparatus and software

Stimuli were generated by a VISAGE graphics card (Cambridge Research Systems, Riverside, Kent, UK) driven by a Dell Precision PC and displayed on a Sony Trinitron F500 flatscreen monitor. Psychophysics software was written in C and C++ and contained embedded VISAGE routines. Psychometric function fitting used routines customized from the Palamedes toolbox (Prins & Kingdom, 2020) running under MATLAB. Graphs were produced in MATLAB.

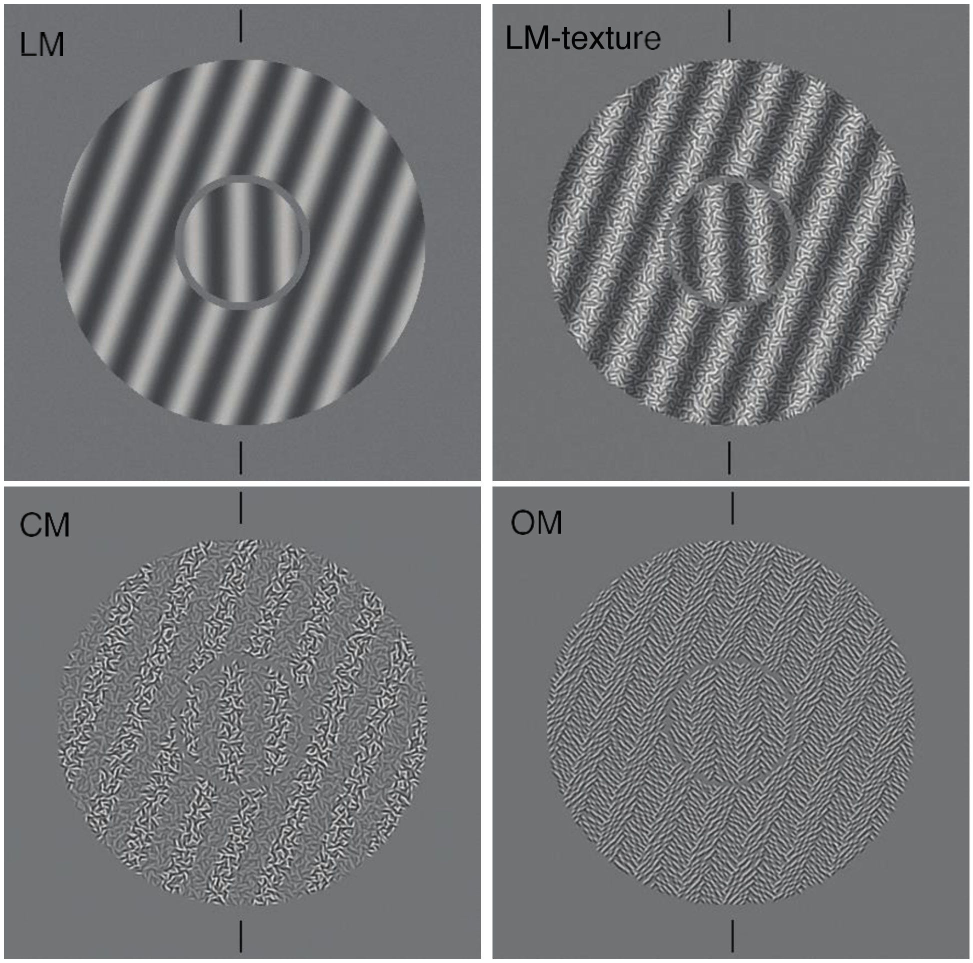

Figure 2.1. Tilt illusion in luminance modulated (LM), luminance modulated with uniform texture (LM-texture), contrast modulated (CM) and orientation-modulated (OM) gratings. The bars in the central test area are physically vertical, but for most observers appear slightly tilted counterclockwise.

Visual Stimuli

Example stimuli are given in Fig. 2. Each stimulus is comprised of a circular central test region 4.0 deg in diameter and a surround annulus of diameter 12 deg, separated by a gap 0.25 deg in width. Modulation frequencies of 4.0, 8.0 and 16.0 cycles-per-image (cpi) were used, which correspond to respectively 0.33, 0.66 and 1.33 cycles per degree (cpd) at the viewing distance of 100 cm. The absolute spatial phases of the stimuli were randomized on each trial, but the spatial-phase relationship between inducer and test was set either to "in-phase" or "antiphase". The two spatial phase relationships, each of which was defined in relation to the randomized absolute phases of inducer and test, must however be understood in context. When the inducer and test were both vertical the in-phase condition resulted in colinear alignment of same-polarity the modulation bars and the anti-phase condition colinear alignment of bars of opposite-polarity. However, as the orientation difference between inducer and test increased the bars in both phase conditions became increasingly misaligned because of the constraints imposed by the geometry of the stimulus and the fact that the spatial frequencies of inducer and test modulations were always kept equal. To have preserved colinear alignment across all inducer-test orientation differences would have required setting the inducer and test to a spatial frequency difference that increased with inducer orientation, therefore compromising the spatial-frequency specificity required in the study.

The LM stimulus, as with the LM component of the LM-texture stimulus, was sinusoidally modulated with a contrast of 0.25 in the first main experiment but with lower contrasts in subsequent experiments as detailed below. The CM and OM stimuli were square-wave modulated to maximize their modulation energy, but we chose not to use square-wave modulation for the LM stimuli in order to avoid the aliasing produced at the sharp edges of the stimulus.

The OM, CM and LM-texture stimuli were comprised of 3600 odd-symmetric Gabor micropatterns with a spatial frequency of 6.0 cpd, a bandwidth at half-height of 1.5 octaves and an envelope diameter of 5 standard deviations (SDs). Gabors were randomly positioned with the constraint that adjacent Gabors were a minimum of 1.7 SDs apart. The orientations of the Gabors were selected from 1400 templates distributed evenly across the 360 deg range, giving an orientation precision of 0.25 deg.

In the CM stimuli the orientations of the Gabors were random, and the contrasts were square-wave modulated with an amplitude of 0.165 and a mean contrast of 0.33. In the OM stimuli the Gabor contrasts were 0.33 and the orientations were square-wave modulated with an amplitude of 45deg around a mean orientation of 90 deg (horizontal).

In the LM-texture stimuli the Gabors and LM stimuli were presented on separate pages of video memory. The Gabor contrasts on one page were sinusoidally modulated with an amplitude of 0.333 and a mean contrast of 0.666, resulting in a peak-to-trough contrast ratio of 3. The LM stimulus on the other page had a modulation contrast of 0.5, resulting also in a peak-to-trough luminance ratio of 3. The Gabor contrast and LM modulations were combined in-phase to simulate a uniform texture subject to luminance-shading modulation (Schofield et al., 2006). The combination was achieved by page-alternating the two modulations at 120 Hz. This halved all contrasts reaching the eye and thus the LM-texture had an LM contrast of 0.25 and Gabor contrasts of 0.333.

Procedure: interleaved sign-of-inducer-orientations

In this study we employ a new method for measuring the TI, one that interleaves two inducers during a session, each of opposite sign but with the same orientation magnitude. The advantage of this method over the single-inducer-orientation method employed in previous studies is twofold. First it reduces any bias to respond according to the perceived inducer orientation: all observers reported that during each session they were largely unaware on each trial as to whether the inducer orientation was oriented clockwise or anticlockwise. Second it allows one to take into account response bias, that is a tendency to respond more clockwise than anticlockwise or vice-versa. By taking the difference between the estimated PSVs for the two opposite-sign inducer orientations (see below) this type of response bias is removed.

In all experiments the observer was presented on each trial with a TI stimulus and tasked with indicating whether the test modulation appeared oriented clockwise or anticlockwise from vertical. Two black lines above and below the stimulus provided a reference to vertical (see Fig. 1). During each session of 100 trials two opposite-sign inducer orientations (e.g. +20deg and -20deg) were presented in random order (50 trials each), and the test orientations were determined by separate staircases for the two inducers to determine for each a point-of-subjective-vertical, or PSV. A "clockwise" response caused a shift in test orientation away from clockwise for the next trial, whereas an "anticlockwise" response caused a shift towards away from anticlockwise for the next trial. The test orientations of each staircase were set at the start of each session to a random value between -6 and +6 deg. For the first 2 trials of each staircase the step size was ±1.25 deg and thereafter ±0.35 deg.

All stimuli were presented in a raised cosine envelope with an exposure duration of 500 msec to minimize the presence of sharp temporal transients. Observers recorded their responses by a key press. Following each response there was an inter-trial-interval of 500ms prior to the next stimulus presentation; hence the observer controlled the timing of stimulus presentation.

Analysis

Data for between 4-8 sessions (400-800 trials) were collected for each condition. The data for the two ±inducer orientations for each condition were separately collated. Data was then pooled into between 5 and 10 "bins". Each bin defined a range of test orientations, with a mean test orientation, number of trials and number of clockwise responses.

Psychometric functions of proportion of clockwise responses against test orientation were fitted with Logistic functions and the PSV was defined as the test orientation giving 0.5 proportion or 50% clockwise responses. The PSV for a given condition was given as half the difference between the clockwise and anticlockwise inducer PSVs to facilitate a comparison with PSVs obtained from previous studies that employed only the single-inducer-per-session method. Error bars on all graphs of individual observers' data are standard errors derived from bootstrap analysis with 400 iterations. Error bars on the averages of observers' data are standard errors of the averages.

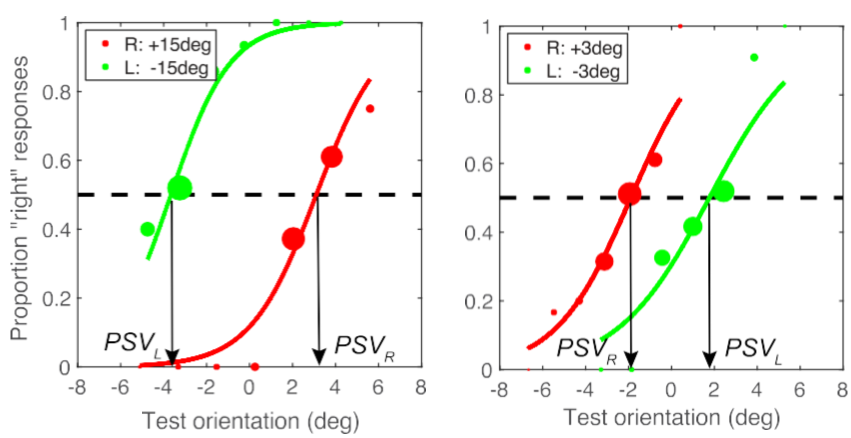

Figure 2.2. Example psychometric functions (PFs) and method for estimating the *PSV* (point-of-subjective-vertical) from our interleaved ± inducer orientation method. Each PF plots the proportion of right, or clockwise responses as a function of the orientation of the test pattern. The diameter of each data point is proportional to the number of trials in each "bin". Continuous curves are Logistic function fits. Red is for the right-leaning or clockwise inducer, green for the left-leaning or anticlockwise inducer. Left graph Observer 2's LM ±15deg inducer; right graph Observer 3's OM ±3deg inducer. Note the reversal in the order of the two PFs in the two graphs. The *PSV* is calculated as $(PSV_R\text{-}PSV_L)/2$, with the resulting positive *PSV* in the left graph indicating repulsion and the negative *PSV* in the righthand graph indicating attraction.

Psychometric function fitting used customized routines from the Palamedes toolbox (Prins & Kingdom, 2018). Fig. 2.2 shows example psychometric functions and illustrates the method for deriving the PSV.

Results

Experiment 1: Tilt illusion for LM, CM and OM gratings

In the first (main) experiment the independent variables were stimulus type (LM, CM, OM), inducer orientation and spatial-phase relationship (in-phase, anti-phase). Modulation frequency was 8 cpi or 0.66 cpd. For the in-phase conditions the following inducer orientations were employed: 0, 1, 3, 5, 7, 10, 15, 20, 30, 40, 50, 60, 70, 80, 90 deg. For the anti-phase conditions the inducer orientations were: 0, 1, 3, 5, 7,1 0, 15, 20, 30, 40, 70 deg. As we noted above the significance of the inducer-test phase relationship declines with inducer-test angle, hence the reduced number of anti-phase orientations beyond the somewhat arbitrary cut-off of 40 deg, albeit with a token inducer of 70deg. Figure 2.3 show the results for respectively the LM, CM and OM stimuli. In each graph PSVs > 0 evidence repulsion whereas PSVs < 0 evidence attraction. For all observers and stimulus types there is clear evidence for the classic TI repulsion effect, with the maximum effect around 10-20deg. There is a hint of a primary attraction effect at around 70 deg in some of the conditions but it is either very weak or non-existent. For both 2nd-order stimuli (OM and CM) robust small angle attraction effects are observed for inducers < 10deg with a maximum effect at approximately 3deg, but no evidence for attraction in this region with the LM stimuli. With the CM stimuli stimuli small angle attraction is found with the in-phase but not anti-phase conditions, whereas with the OM stimuli it is found with both phases, but more so with the in-phase condition.

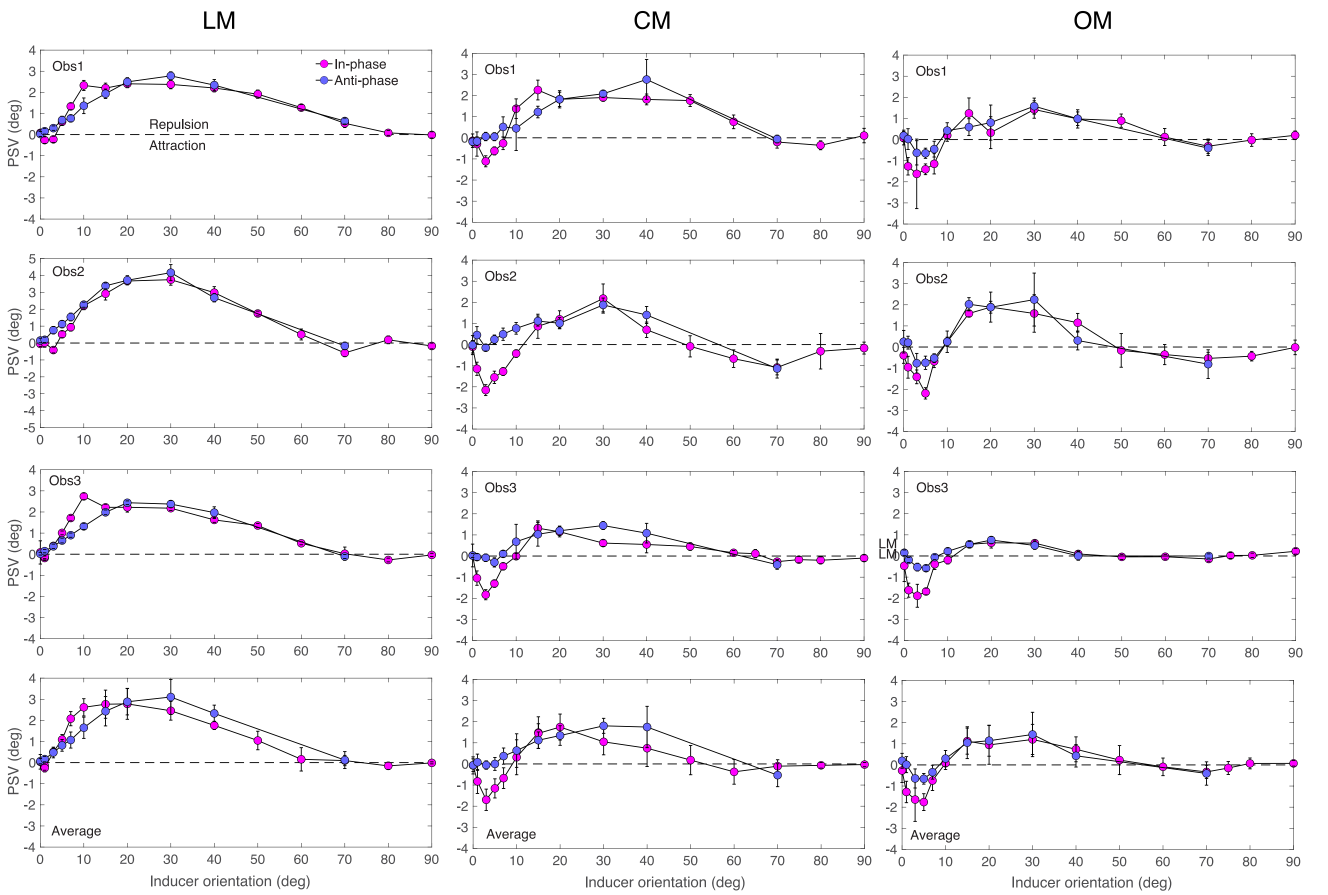

Figure 2.3. PSVs (points of subjective vertical) as a function of absolute inducer orientation for 3 observers, plus the average across observers, for the luminance-modulated (LM), contrast modulated (CM) and orientation modulated (OM) stimuli. Magenta symbols are for in-phase, blue symbols for anti-phase conditions. PSVs > 0 show repulsion, PSVs < 0 attraction. Note that the Y axis range for Observer 2's LM data is -5 to +5 compared with the -4 to + 4 range in all other graphs. Small-angle attraction is readily observed in the CM and OM stimuli. Error bars for the individual observers' data are standard errors derived from bootstrap analysis. Error bars for the Average data are derived by combining observers' PSVs with the bootstrap errors using Cochrane's method (https://www.statstodo.com/CombineMeansSDs.php).

Experiment 2: Sine-wave versus square-wave OM modulations

In what follows we consider three possible reasons for the absence of small angle attraction with our LM stimuli. First, it is possible that it is because our LM stimuli were sinusoidally modulated whereas our CM and OM stimuli were square-wave modulated. A second possibility is that, unlike with our LM stimuli, our CM and OM stimuli were constructed from micropatterns. A third possibility is because the effective contrast of our LM patterns was higher than that of our CM and OM patterns. Each of these possibilities will be considered in turn.

If the absence of small-angle attraction in the LM stimulus is a result of using a sine-wave rather than square-wave modulation then we should expect secondary attraction to disappear with the use of sine-wave modulation of the OM stimulus. We chose to test this condition rather than introduce square-wave modulation to the LM stimulus because of the aliasing problem described earlier with square-wave LM.

Figure 2.4 shows the results for both sine-wave and square-wave OM modulations for just the 3 deg and 15 deg inducers, the approximate orientations for respectively the maximum secondary attraction and repulsion effects. Data for both in-phase and anti-phase conditions, and for 3 modulation spatial frequencies are provided. Results show that both secondary attraction and repulsion occur with sine-wave modulation.

Experiment 3: LM versus LM-texture

To test whether it is the presence of micropatterns in the stimulus that promotes small-angle attraction we compare results for the LM and LM-texture stimuli. Figure 2.5 shows results for 3deg and 15deg, in-phase and anti-phase, 3 spatial-frequency conditions. The two key findings are that 1. the attraction effect is present for all in-phase LM-texture conditions, and 2. the attraction effect is now present in the lowest spatial-frequency (4 cpi) LM condition. These results suggest that defining the waveform by micropatterns is at least part of the reason for the secondary attraction effect revealed in the present study. We will return to this finding later.

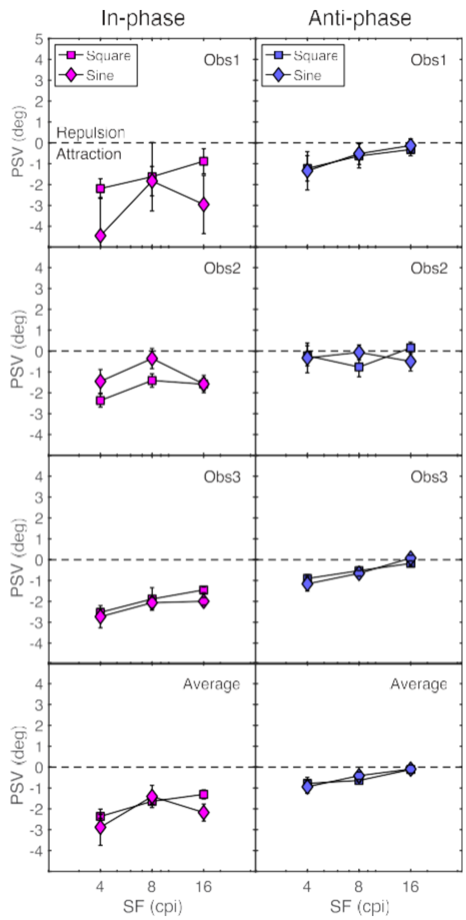

Figure 2.4. PSVs for 3 subjects as a function of modulation spatial frequency (SF) for 3 deg inducers for square-wave (square symbols) and sine-wave (diamond symbols) OM. Upper panels and magenta symbols are for the in-phase and lower panels and blue symbols for the anti-phase conditions. Errors on individual data points are standard errors derived from bootstrap analysis, while errors for the Average data in the bottom panels are standard errors calculated from the observers' PSVs.

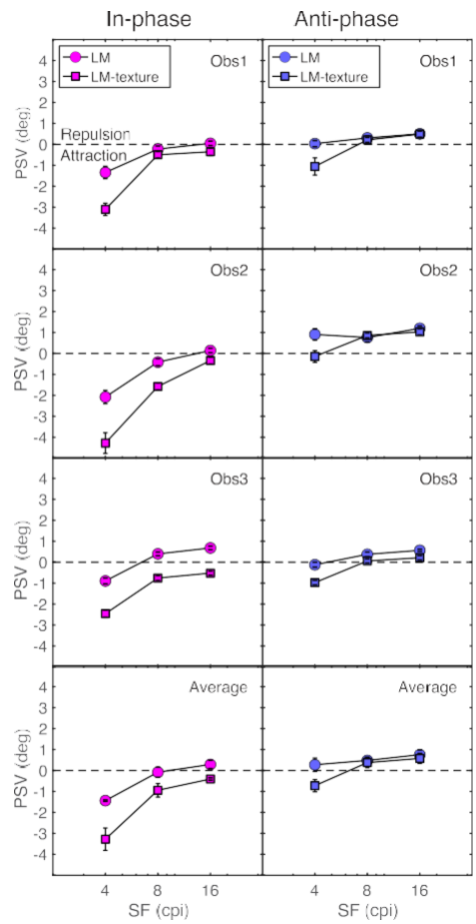

Figure 2.5. PSVs for LM and LM-texture stimuli as a function of spatial-frequency and spatial phase for 3deg inducers. Errors are as described for Fig. 4.

Experiment 4: TI with low versus high contrast LM

As discussed above it is possible that secondary attraction is a phenomenon that only occurs with low-contrast gratings and that the "effective" contrast of the OM and CM modulations is simply lower than that of the LM stimuli. To test for this possibility we generated LM stimuli with contrasts that were "equivalent" to those employed with the OM stimuli. It makes intuitive sense that "equivalence" in our case should be in terms of the nature of the task used in our experiments, i.e. orientation discriminability. Orientation discriminability in our experiments is given by the slopes of the psychometric functions so for this experiment we determined the contrast of the LM stimuli that produced the same psychometric function slopes as the OM stimuli. We determined these slopes using the same task as in the main experiments but in the absence of inducer modulations as we found that the slopes were strongly affected by inducer orientation. First we measured the OM slope using the same test modulation as in the main experiment, then we measured slopes for various LM test contrasts. To determine the equivalent LM contrast we used linear interpolation of the LM slope-versus contrast function to find the slope that matched that of the OM stimulus. The resulting equivalent LM contrasts were, for the observers 1-4 used in this study, respectively: a, b, c, d. Results for the low, equivalent LM contrasts alongside the 0.25 LM contrast condition from the first experiment are shown in Fig. 2.6. Although there is a degree of variability across observers the overall trend is towards greater small-angle attraction for the low, equivalent LM contrast condition.

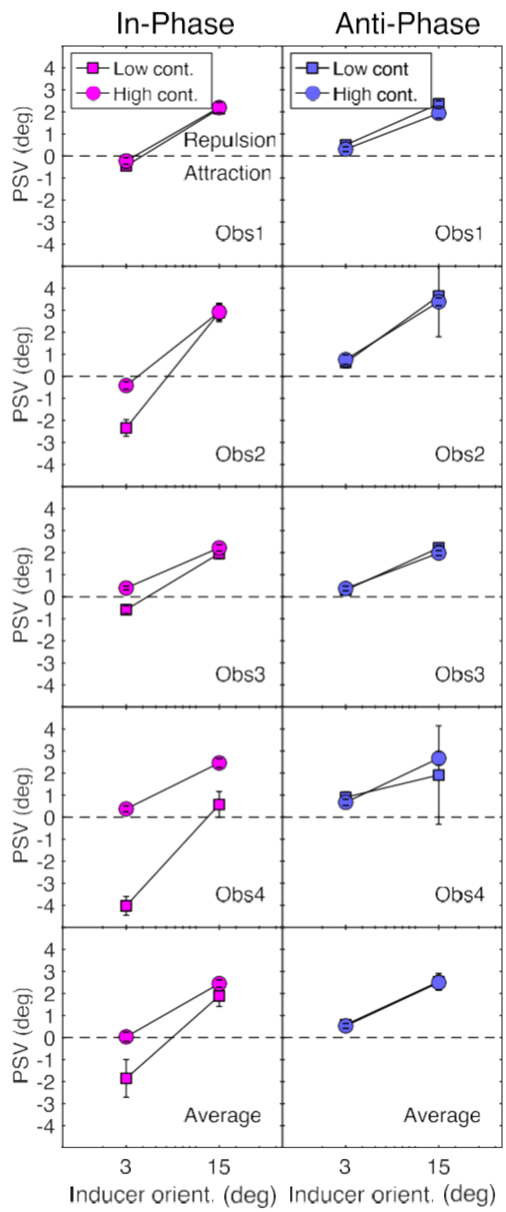

Figure 2.6. Effect of contrast on the PSVs with LM stimuli, as a function of inducer orientation (orient.) and phase, for four observers. See text for further details. Errors are as described for Fig. 4.

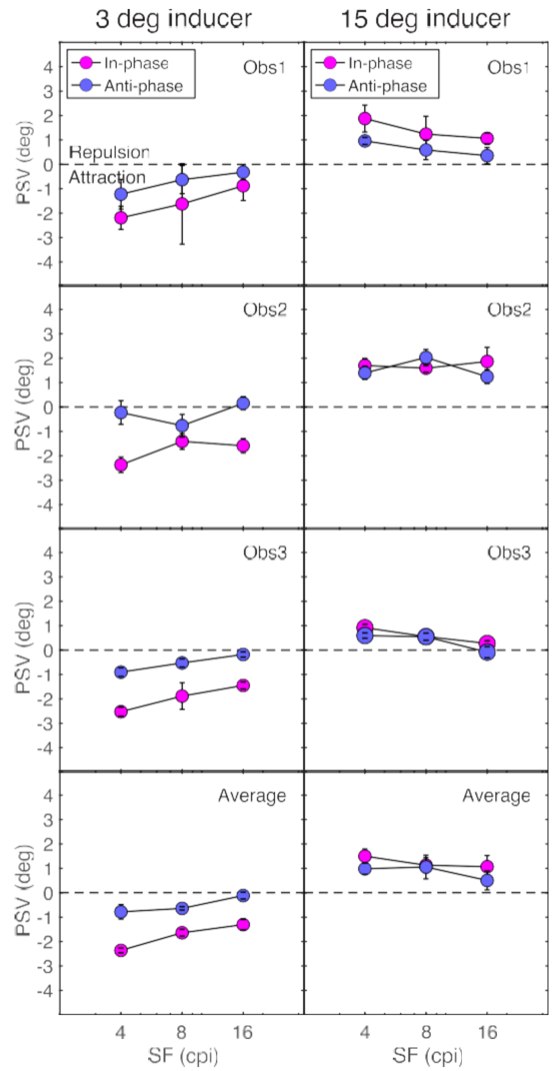

Figure 2.7. Effect of spatial frequency of PSVs with square-wave OM stimuli, for both 3deg (left panel) and 15 deg (right panel) inducers. Errors are as described for Fig. 4.

Experiment 5: Small-angle attraction versus repulsion across spatial frequency

Earlier, Figs. 2.4 and 2.5 showed the effect of spatial-frequency on the TI with 3 deg inducers. The trend is clearly towards a decline in small-angle attraction with increasing spatial frequency. Do we obtain a similar trend with the repulsion effect? Fig. 2.7 compares the results from Fig. 2.4's OM square-wave TI with 15 deg repulsion data using the same stimulus. One can see that as with the 3 deg attraction data the 15 deg repulsion data shows a similar decline in TI magnitude with spatial frequency.

Experiment 6: Effect of gap width

Previous studies have shown that increasing the width of the gap between test and inducer reduces the repulsion effect in the TI (Mareschal & Clifford, 2012). In this experiment we compare the effect of gap width on both the attraction and repulsion effects using respectively 3 deg. and 15 deg. inducers with the OM stimulus. Results are shown in Figure 2.8. The highest attraction effect at 3 deg. has been obtained when the stimuli were presented with 0.25 gap width and again the largest repulsion effect at 15 degree has been obtained at this lowest gap width. The results show similar proportional declines of the TI with gap width for all conditions, with the elimination of TI at a gap width of 1-2 deg.

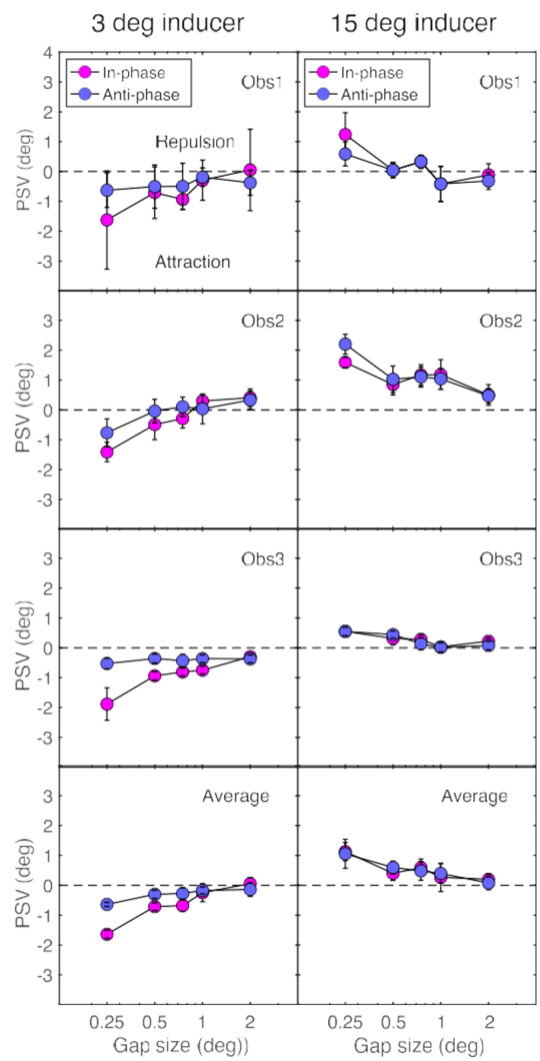

Figure 2.8. PSVs as a function of gap width for 3deg and 15deg inducers with OM. In-phase results shown with magenta, anti-phase with blue symbols. Errors are as described for Fig. 2.4.

Discussion

Small-angle attraction in the tilt illusion

We have demonstrated small-angle attraction in the TI at inducer orientations <10 deg in CM, OM and LM-texture stimuli, LM stimuli of relatively low-spatial-frequency, and in some subjects LM stimuli of equivalent (i.e. very low) contrast. With the in-phase inducer-test modulations the magnitude of small angle attraction was in general as strong or even stronger than the repulsion effect observed at relatively large angles.

What mechanism underpins small angle attraction in the TI? Numerous studies have shown a decline in the TI as inducer and test orientations approach each other (e.g. see our own results with LM stimuli in Fig. 2.2). This speaks to a decline in the amount of inhibition among orientation-selective neurons as the difference in their orientation preferences approaches zero, a feature that is embodied in models of the TI as well as related phenomena (Clifford, 2014; Motoyoshi & Kingdom, 2003). While an absence of inhibition is presumably a pre-condition for the small-angle attraction in the TI observed here, it is arguably insufficient. Moreover, the disinhibition theory advanced to account for the large-angle attraction effect in the TI (Clifford, 2014) seems an unlikely explanation for its small-angle relative. If one thinks of small-angle attraction in the TI as an example of the classical notion of assimilation, it is best explained as a consequence of a blending of the receptive fields of the inducer- and test-sensitive neurons, which will have the effect of shifting the test stimulus's neural population response towards that of the inducer's.

Five pieces of evidence attest to this explanation. First, the anti-phase conditions produced either none or reduced small-angle attraction compared to the in-phase conditions, presumably because of mutual cancelation of the inducer's and test's receptive fields in the region of the display where they overlapped. Second for the fixed-size test area employed in the present study the small-angle attraction increased as spatial frequency decreased, consistent with the idea that the larger receptive fields associated with lower spatial frequencies would have enjoyed greater receptive field overlap. Third, in keeping with previous findings by Virsu and Taskinen (1975) and Mareschal and Clifford (2012) in relation to the repulsion effect, the small-angle attraction declined markedly with gap size, disappearing altogether between 1-2 deg, as one would expect if the amount of receptive field overlap also declined with gap size. Fourth, though not immediately obvious, is the effect of reducing LM contrast. Note that the "equivalent" LM contrasts employed in this manipulation were selected to match the orientation discriminability of the OM stimuli, and were found to be very low, ranging from about 1-5% across observers, with the result that at the low end of the range the stimulus was barely visible. At such low contrasts there is good evidence from single-unit recording of neurons in the macaque that the size of receptive fields can increase by 2-4 times their normal size (Sceniak et al., 1999; Kapadia, Westheimer & Gilbert, 1999), a finding that resonates with psychophysical evidence obtained from orientation discrimination in the context of surround masks (Mareschal, Henrie & Shapley, 2002). Finally we have the greater small-angle attraction effect obtained for LM-texture compared to LM stimuli at all spatial frequencies. This is in keeping with the idea that the presence of micropatterns in the LM-texture stimulus has the effect of broadening the range of orientation and spatial-frequency channels sensitive to the LM modulation component in the stimulus.

Whatever happened to large-angle attraction?

One interesting feature of data is the almost complete absence of the attraction effect typically found with large angles around 70 deg. The large-angle attraction effect has been attributed to disinhibition (Clifford, 2014) but other accounts have also been put forward. Based on the finding that large-angle attraction effects are subject to different spatio-temporal dependencies compared to the repulsion effect, some authors have suggested that it is attraction effect is mediated by higher striate areas where orientation constancy mechanisms are involved (Wenderoth and Johnstone, 1987, 1988; Zwan and Wenderoth, 1994, 1995; Smith and Wenderoth 1999). Consistent also with this account is the evidence from Tomassini & Solomon (2014) that the large-angle attraction effect requires conscious awareness (though see the contrary finding by an earlier report by Mareschal & Clifford, 2012). The need for conscious awareness to elicit large-angle attraction would be consistent with the effect of interleaved opposite-sign-of-angle inducers within each session, as we did here. We noted earlier that our observers reported being unaware of the sign of inducer angle on each trial during a session. Consistent with this suggestion is unpublished data where we find greater large-angle attraction with our stimuli when using the traditional single-sign-of-angle method.

Conclusions

We have demonstrated the presence of a strong attractive effect in the Tilt Illusion (TI) for small inducer-test orientation differences (<10deg) in two types of 2nd-order stimuli, namely contrast modulated (CM) and orientation modulated (OM) patterns, and in 1st-order luminance modulated (LM) stimuli made either from micropatterns or presented at a relatively low spatial frequency. Our measurements of the strength of both the attraction and repulsion effects in the

TI across a range of conditions (type of modulation, inducer-test spatial-phase relationships, modulation spatial frequency, modulation shape, inducer-test gap width) have revealed the conditions that support the existence of both effects and in doing so have advanced our understanding of the underlying mechanisms of the Tilt Illusion.

Acknowledgements

We thank Drs. Curtis Baker and Alex Baldwin for helpful discussions, and Dr. Nicolas Prins for advice concerning the method for deriving standard errors from observer-averaged data. This work was supported by a Natural Sciences and Engineering Research Council grant #RGPIN-2016-03915 given to FK.

Chapter 3: General Discussion

Summary of thesis findings

This thesis has demonstrated a new phenomenon in relation to a particular contextual effect in visual texture perception known as the tilt illusion (TI). Experiments have demonstrated for the first time the presence of small-angle attraction in the TI with 2nd-order contrast modulated (CM) and orientation modulated (OM) gratings, as well as in 1st-order luminance modulated (LM) gratings that are either relatively low in spatial frequency, low in contrast or contain added perceptually uniform texture. I find that small-angle attraction is dependent on the spatial-phase relationship between inducer and test, in general greater when the two are in-phase rather than in antiphase. Both the small-angle attraction and more conventional repulsion effect declines with the size of the gap between inducers and test, disappearing altogether by about 1 deg.

Relation to previous studies

The repulsion effects measured here are consistent with all previous TI reports, in that I find the strongest repulsion between 15 and 30 degrees. On the other hand the weak, or non-existent large-angle attraction effect in my data is inconsistent with most previous studies that find significant amounts of large-angle attraction around 70 degrees (e.g., Over, Broerse, & Crassini, 1972; Wenderoth & Johnstone, 1987). In Chapter 2, I considered a possible reason for the near-absence of large-angle attraction in my data is the method I employed of interleaving positive and negative signs of inducer angle during each session. My rationale for using this method was that it likely minimized any conscious bias towards making judgments based on inducer angle, and, by taking the difference between the two PSVs (point-of-subjective-vertical) estimated for the different angle signs, removed any response bias towards judging the test grating as left- as opposed to right-oblique. However this method may come with a cost. If large-angle attraction is dependent on conscious awareness as has been suggested (Tomassini & Solomon (2014; though see a report to the contrary by Mareschal & Clifford, 2012), then the near-absence of large-angle attraction was a result of my subjects being largely unaware on each trial of the inducer sign, as they indeed reported. Some support for this comes from unpublished preliminary data using the traditional single-sign-of-inducer method applied to the same stimuli as used in this study, where I find a greater amount of large-angle attraction.

With regard to the main finding of the thesis, the small-angle attraction effect I have revealed in the TI resonates most closely with the findings of Blake et al. (1985) in their study of overlay masking - their Figs. 1 and 2 look remarkably similar to the in-phase CM and OM plots in Fig. 2.3 of the previous chapter. As a reminder, Blake et al., using orientationally narrowband luminance noise patterns, measured the apparent tilt of a "test" pattern in the presence of a superimposed "mask" pattern, and while finding repulsion across most of the range found significant amounts of attraction at 5 degrees. Although at first I only found small-angle attraction in my CM and OM stimuli I later went on to show that small-angle attraction does occur with LM gratings under certain conditions, in keeping with Blake et al.'s masking results.

Why small-angle attraction?

In relation to the small-angle attraction that Blake et al. found at 5 deg, the authors suggested that "… the pattern of neural activity produced by a pair of orientations differing by onlya few degrees resembles the pattern of activity produced by a single orientation situated somewhere between the pair" (page 1475). In other words what they are suggesting is that the pattern of activity of the neurons in response to the mask and test blend at small angle differences, and are thus interpreted "as if" a stimulus mid-way between the two is present. This is an example therefore of what is traditionally termed "assimilation". Assimilation is found in a variety of domains of visual perception, but most notably in the domain of color vision where there are many examples of "color assimilation" (reviewed by Kingdom, 2017). One example is given here in Fig. 3.1.

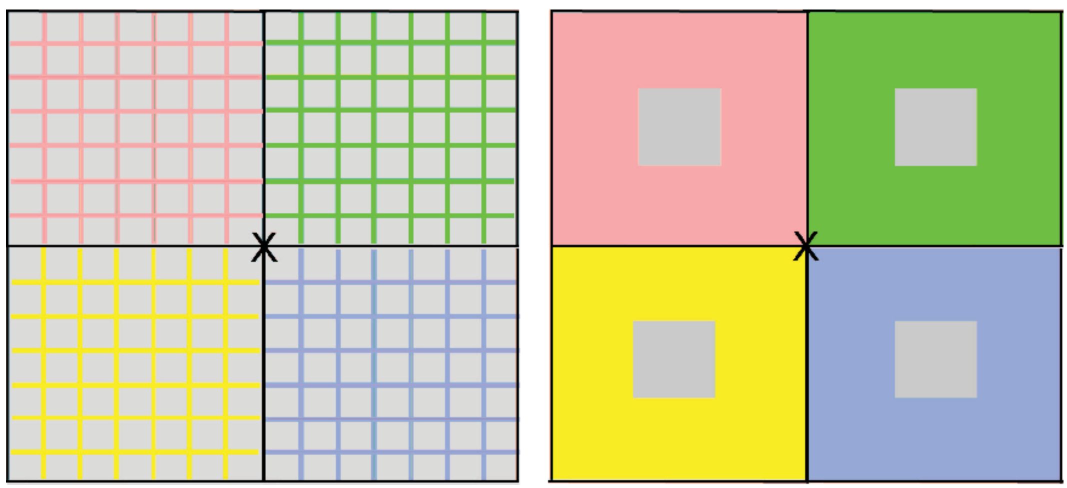

Figure 3.1. Color assimilation (left) and color contrast (right). In the left figure the grid lines induce a desaturated tint of same color into the grey background, whereas in the right figure the background induces a desaturated complementary color into the central grey patch. Both effects are enhanced by fixation of the central crosses. The assimilation and contrast effects in color are analogous to the attraction and repulsion effects in the tilt illusion. Figure taken from Fig. 1 of Kingdom (2017).

The standard explanation for color assimilation is that it occurs when two or more different colored regions fall within the receptive fields of color-sensitive neurons, but when there are no neurons available with receptive fields small enough to resolve the colors. As a result the colors appear to spread into each other. In the case of the small-angle attraction demonstrated in this thesis, the analogous explanation is thus. The receptive fields of the neurons sensitive to the test region will tend to carry over into the inducer region, and in the absence of inhibitory interactions between the inducer and test sensitive neurons, the range of neurons sensitive to the test region will include those sensitive to the inducer. The result is that population response of neurons to the test region will be slightly skewed towards that of the inducer orientation, causing the test orientation to appear shifted towards that of the inducer orientation.

As pointed out in Chapter 2 the five pieces of evidence in support of this explanation are that the small-angle attraction effect a) is dependent, wholly or in part, on the spatial-phase relationship between test and inducer; b) is greater at relatively low spatial frequencies (assuming a fixed size test region); c) in the case of LM stimuli greater at low contrasts; d) in the case of LM stimuli greater with added perceptually uniform texture; e) disappears when the gap between inducer and test increases to 1-2 degrees. All these findings are consistent with the idea that the amount of small-angle attraction is determined by the extent of overlap between the receptive fields of inducer and test neurons.

Leaving aside for the moment the spatial-phase dependency of small-angle attraction in the above list, the spatial-frequency dependency follows naturally from the fact that for a fixed-size test area, the neural receptive-fields will increase and therefore more overlap as spatial frequency decreases. Perhaps less obvious are the putative effects on receptive-field overlap in the LM stimuli of reducing contrast and adding uniform texture. To begin with let us not forget that the “equivalent” LM contrasts that were employed to match the orientation discriminability of the OM stimuli were very low – ranging from about 1-5% across observers, which means that at the low end of the range the stimulus was barely visible. At such low contrasts there is good evidence from single-unit recording of neurons in the macaque that the size of receptive fields can increase by 2-4 times of their normal size (Sceniak et al., 1999; Kapadia, Westheimer & Gilbert, 1999), a finding that resonates with psychophysical evidence obtained from orientation discrimination in the context of surround masks (Mareschal, Henrie & Shapley, 2002).

With regard to the effect of adding texture to the LM stimuli on the magnitude of small-angle attraction, one must first add a note of caution. The LM-texture stimulus was generated by adding a CM to an LM grating, such that the peaks of the CM coincided with the peaks of the LM. In so doing the physical contrasts of the micropatterns in the CM stimulus became uniform across the waveform. However, it is not necessarily the case that this meant that the micropatterns were *perceptually* uniform in contrast, because there may have been unforeseen nonlinearities in the LM + CM combination. As a result the ostensibly "pure" LM-texture stimulus might have been contaminated with a perceptual contrast modulation that was responsible wholly or in part for eliciting the small-angle attraction observed in the data. With this caveat in mind the most likely reason why the LM-texture produced small-angle attraction is because the micropattern texture spread out the Fourier energy in the stimulus thus stimulating a wider range, and hence larger set of neural receptive field sizes.

One interesting and somewhat unexpected result is that both repulsion and small-angle attraction affects in the OM stimuli were equally disrupted by the introduction of a gap between the inducer and test, with both effects disappearing between 1-2 deg. This limit corresponds to 0.66-1.3 cycles of the 0.66 cpd grating used in the gap experiment, which is in keeping with the receptive field bandwidths of cortical 2nd-order-sensitive neurons (Mareschal & Baker, 1998). While this result is perfectly in keeping with the receptive-field overlap explanation for the small-angle attraction, it also suggests that the repulsion effects is at least partially due to inhibitory interactions between overlapping inducer and test receptive fields, in keeping with the overlay masking repulsion effects found by Blake et al. (1985).

Future directions

A key finding of this thesis is that the small-angle attraction we observed was dependent on the spatial-phase relationship between inducer and test. However, as I pointed out in Chapter 2, keeping the inducer and test gratings in phase alignment was only possible at small inducer-test angular differences: at medium-to-large angular differences the pre-requisite of keeping the spatial frequencies of inducer and test the same precluded the possibility of such phase alignment. To explore the effect of relatively large inducer-test angular differences on the TI with consistent phase alignment requires a different type of stimulus geometry, one in which the relative spatial frequency of inducer and test was a function of their angular difference. It would be interesting to test whether the attraction effect found here for small angles extends to medium and large angles using such a stimulus arrangement.

The inducer-test small-angle attraction effect might not be restricted to the orientation domain. For example, it might also be found with other types of 2nd-order stimuli, for example spatial-frequency-modulated, stereo-disparity-modulated and motion-modulated stimuli, all of which could be explored in future studies.

Conclusions

In this thesis I observed a robust attraction effect in the tilt illusion (TI) for small inducer-test orientation differences (<10deg) in two types of 2nd-order stimuli - contrast modulated (CM) and orientation modulated (OM), as well as in 1st-order luminance modulated (LM) stimuli made either from micropatterns, presented at relatively low spatial frequencies or at low contrasts. I suggest that the reason for such small-angle attraction is a combination of the absence of inhibitory interactions between inducer and test at small angular differences, together with the presence of overlapping inducer and test neural receptive fields in the region of the test stimulus. The overall significance of our findings is that they add one more dimension to the variety of contextual effects observed in the processing of both 1st- and 2nd-order stimuli, and hence to my understanding of the underlying visual mechanisms responsible for contextual effects as a whole.

References

Badcock, D., & Hutchison, H. (1998). Orientation dependent interaction between first-and second-order texture properties. In *Orientation dependent interaction between first-and second-order texture properties* (p. s858). Association for Research in Vision and Ophthalmology (ARVO).

Baker, C. L. (1999). Central neural mechanisms for detecting second-order motion. *Current opinion in neurobiology*, *9*(4), 461-466.

Bergen, J. R., & Adelson, E. H. (1988). Early vision and texture perception. *Nature*, *333*(6171), 363-364.

Blake, R., Holopigian, K., & Jauch, M. (1985). Another visual illusion involving orientation. *Vision research*, *25*(10), 1469-1476.

Blakemore, C., Carpenter, R. H., & Georgeson, M. A. (1970). Lateral inhibition between orientation detectors in the human visual system. *Nature*, *228*(5266), 37-39.

Cannon, M. W., & Fullenkamp, S. C. (1991). Spatial interactions in apparent contrast: inhibitory effects among grating patterns of different spatial frequencies, spatial positions and orientations. *Vision research*, *31*(11), 1985-1998.

Cant, J. S., Arnott, S. R., & Goodale, M. A. (2009). fMR-adaptation reveals separate processing regions for the perception of form and texture in the human ventral stream. *Experimental Brain Research*, *192*(3), 391-405.

Cavina-Pratesi, C., Kentridge, R. W., Heywood, C. A., & Milner, A. D. (2010a). Separate processing of texture and form in the ventral stream: evidence from FMRI and visual agnosia. *Cerebral Cortex*, *20*(2), 433-446.

Cavina-Pratesi, C., Kentridge, R. W., Heywood, C. A., & Milner, A. D. (2010b). Separate channels for processing form, texture, and color: evidence from FMRI adaptation and visual object agnosia. *Cerebral Cortex, 20*(10), 2319–2332.

Chubb, C., & Landy, M. S. (1991). Orthogonal distribution analysis: A new approach to the study of texture perception. In M. S. Landy & J. A. Movshon (Eds.), Computational Models of Visual Processing (pp. 291–301). Cambridge, MA: MIT Press.

Chubb, C., Sperling, G., & Solomon, J. A. (1989). Texture interactions determine perceived contrast. *Proceedings of the National Academy of Sciences*, *86*(23), 9631-9635.

Clifford, C. W. (2014). The tilt illusion: Phenomenology and functional implications. *Vision research*, *104*, 3-11.

Cruickshank, A. G., & Schofield, A. J. (2005). Transfer of tilt after-effects between second-order cues. *Spatial Vision*, *18*(4), 379-397.

El-Shamayleh, Y., & Movshon, J. A. (2011). Neuronal responses to texture-defined form in macaque visual area V2. *Journal of Neuroscience, 31*, 8543–8555.

Filangieri, C., & Li, A. (2009). Three-dimensional shape from second-order orientation flows. *Vision Research,* 49(11), 1465–1471.

Georgeson, M. A. (1973). Spatial frequency selectivity of a visual tilt illusion. *Nature, 245*(5419), 43–45.

Gibson, J. J. (1937). Adaptation, after-effect, and contrast in the perception of tilted lines. II. Simultaneous contrast and the areal restriction of the after-effect. *Journal of Experimental Psychology*, *20*(6), 553.

Gillam, B. (1998). Illusions at century's end. *Perception and cognition at century's end*, 95-136.

Gregory, R. L. (1997). Visual illusions classified. *Trends in cognitive sciences*, *1*(5), 190-194.

Gregory, R. L. (2004). The oxford companion to the mind (oxford companions) (2nd ed.). Oxford University Press.

Hallum, L. E., Landy, M. S., & Heeger, D. J. (2011). Human primary visual cortex (V1) is selective for second-order spatial frequency. *Journal of Neurophysiology*, *105*(5), 2121-2131.

Hering, E. (1874/1964). Outlines of a theory of the light sense. (L.M.H.D. Jameson, Trans.). Cambridge, MA: Harvard University Press.

Kapadia, M. K., Westheimer, G., & Gilbert, C. D. (1999). Dynamics of spatial summation in primary visual cortex of alert monkeys. *Proceedings of the National Academy of Sciences*, *96*(21), 12073-12078.

Kingdom F. A. A. (2015). Visual Illusions, Models of. In Encyclopedia of Computational Neuroscience, by Jaeger D, Jung R (Eds.), Vol. 4, pp. 3072-3087. Springer, New York, Heidelberg, Dordrecht, London.

Kingdom, F. A. A. (2017). Colour assimilation. In *The Oxford Compendium of Visual Illusions*, by Shapiro, A. G. & Todorovic, D. (Eds.). Oxford University Press: Oxford.

Kingdom, F. A., Keeble, D., & Moulden, B. (1995). Sensitivity to orientation modulation in micropattern-based textures. *Vision research*, *35*(1), 79-91.

Langley, K., Fleet, D., & Hibbard, P. (1996). Linear filtering precedes nonlinear processing in early vision. *Current Biology, 6*(7), 891–896.

Larsson, J., Landy, M. S., & Heeger, D. J. (2006). Orientation-selective adaptation to first-and second-order patterns in human visual cortex. *Journal of neurophysiology*, *95*(2), 862-881.

Lin, L. M., & Wilson, H. R. (1996). Fourier and non-fourier pattern discrimination compared. *Vision Research, 36*(13), 1907–1918.

Mareschal, I., & Baker, C. L. (1998a). A cortical locus for the processing of contrast-defined contours. *Nature Neuroscience, 1*(2), 150–154.

Mareschal, I., & Baker, C. L. (1998b). Temporal and spatial response to second-order stimuli in cat area 18. *Journal of Neurophysiology, 80*(6), 2811–2823.

Mareschal, I., & Clifford, C. (2012). Dynamics of unconscious contextual effects in orientation processing. *Journal of Vision*, 12(9), 7553–7558.

Mareschal, I., Henrie, J. A., & Shapley, R. M. (2002). A psychophysical correlate of contrast dependent changes in receptive field properties. *Vision Research*, *42*(15), 1879-1887.

Mareschal, I., Morgan, M. J., & Solomon, J. A. (2010). Cortical distance determines whether flankers cause crowding or the tilt illusion. *Journal of Vision, 10*(8), 13-13.

Montaser-Kouhsari, L., Landy, M. S., Heeger, D. J., & Larsson, J. (2007). Orientation-selective adaptation to illusory contours in human visual cortex. *Journal of Neuroscience*, *27*(9), 2186-2195.

Motoyoshi, I., & Kingdom, F. A. (2003). Orientation opponency in human vision revealed by energy-frequency analysis. *Vision Research*, *43*(21), 2197-2205.

Muller-Lyer, F. C. (1889). Optische urteilstauschungen. *Archiv fur Anatomie und Physiologie, Physiologische Abteilung*, *2*, 263-270.

Over, R., Broerse, J., & Crassini, B. (1972). Orientation illusion and masking in central and peripheral vision. *Journal of experimental psychology*, *96*(1), 25-31.

Prins, N. (2018). Applying the model-comparison approach to test specific research hypotheses in psychophysical research using the Palamedes toolbox. *Frontiers in psychology*, *9*, 1250.

Ringach, D. L. (1998). Tuning of orientation detectors in human vision. *Vision Research, 38*(7), 963–972.

Sceniak, M. P., Ringach, D. L., Hawken, M. J., & Shapley, R. (1999). Contrast's effect on spatial summation by macaque V1 neurons. *Nature neuroscience*, *2*(8), 733-739.

Schofield, A. J., & Georgeson, M. A. (1999). Sensitivity to modulations of luminance and contrast in visual white noise: Separate mechanisms with similar behaviour. *Vision Research*, *39*(16), 2697-2716.

Schofield, A. J. (2000). What does second-order vision see in an image?. *Perception*, *29*(9), 1071-1086.

Schofield, A. J., Hesse, G., Rock, P. B., & Georgeson, M. A. (2006). Local luminance amplitude modulates the interpretation of shape-from-shading in textured surfaces. *Vision Research*, *46*(20), 3462-3482.

Smith, S., & Wenderoth, P. (1999). Large repulsion, but not attraction, tilt illusions occur when stimulus parameters selectively favour either transient (M-like) or sustained (P-like) mechanisms. *Vision Research, 39*(24), 4113–4121.

Smith, S., Clifford, C. W., & Wenderoth, P. (2001). Interaction between first- and second-order orientation channels revealed by the tilt illusion: Psychophysics and computational modelling. *Vision Research*, 41(8), 1057–1071.

Snowden, R. J., & Hammett, S. T. (1998). The effects of surround contrast on contrast thresholds, perceived contrast and contrast discrimination. *Vision research*, *38*(13), 1935-1945.

Stylianou-Korsnes, M., Reiner, M., Magnussen, S. J., & Feldman, M. W. (2010). Visual recognition of shapes and textures: an fMRi study. *Brain Structure and Function*, *214*(4), 355-359.

Takao, S., Watanabe, K. & Clifford, C. W. G. (2020). Angular tuning of tilt illusion depends on stimulus duration. *Vision Research,* 175, 85-89.

Tolhurst, D. J., & Thompson, P. G. (1975). Orientation illusions and after-effects: Inhibition between channels. *Vision research*, *15*(8-9), 967-972.

Tomassini, A., & Solomon, J. A. (2014). Awareness is the key to attraction: Dissociating the tilt illusions via conscious perception. *Journal of vision*, *14*(12), 15-15.

van der Zwan, R., & Wenderoth, P. (1994). Psychophysical evidence for area v2 involvement in the reduction of subjective contour tilt aftereffects by binocular rivalry. *Visual Neuroscience*, *11*(4), 823–830.

van der Zwan, R., & Wenderoth, P. (1995). Mechanisms of purely subjective contour tilt aftereffects. *Vision Research, 35*(18), 2547–2557.

Virsu, V., & Taskinen, H. (1975). Central inhibitory interactions in human vision. *Experimental Brain Research*, *23*(1), 65-74.

Wade, N. J. (2006). *Perception and illusion: Historical perspectives*. Springer Science & Business Media.

Wallace, G. K. (1969). The critical distance of interaction in the zöllner illusion. *Perception & Psychophysics, 5*(5), 261–264.

Wenderoth, P., & Johnstone, S. (1987). Possible neural substrates for orientation analysis and perception. *Perception, 16*(6), 693–709.

Wenderoth, P., & Johnstone, S. (1988). The different mechanisms of the direct and indirect tilt illusions. *Vision Research*, *28*(2), 301–312.

Wilson, H. R., Ferrera, V. P., & Yo, C. (1992). A psychophysically motivated model for twodimensional motion perception. *Visual Neuroscience, 9*(1), 79–97.

Xing, J., & Heeger, D. J. (2000). Center-surround interactions in foveal and peripheral vision. *Vision research*, *40*(22), 3065-3072.